SIAM J. SCI. COMPUT.
Vol. 22, No. 6, pp. 2256–2281

HIGH RESOLUTION SCHEMES FOR CONSERVATION LAWS WITH LOCALLY VARYING TIME STEPS*

CLINT DAWSON† AND ROBERT KIRBY†

Abstract. We develop upwind methods which use limited high resolution corrections in the spatial discretization and local time stepping for forward Euler and second order time discretizations. L^∞ stability is proven for both time stepping schemes for problems in one space dimension. These methods are restricted by a local CFL condition rather than the traditional global CFL condition, allowing local time refinement to be coupled with local spatial refinement. Numerical evidence demonstrates the stability and accuracy of the methods for problems in both one and two space dimensions.

Key words. spatially varying time steps, upwinding, conservation laws

AMS subject classifications. 35L65, 65M12, 65M30

PII. S1064827500367737

1. Introduction.

Hyperbolic conservation laws model a wide range of physically interesting phenomena such as gas dynamics, shallow water flow, and advection of contaminants. Conservative high resolution methods with explicit time discretization have proven effective in capturing the sharp, moving fronts common in these applications. It is well known that such methods require the time step to satisfy a CFL condition in order to guarantee stability.

Local spatial refinement is often introduced in order to resolve these fronts more efficiently. However, this local refinement reduces the allowable time step for the explicit time discretizations typically employed. Rather than considering a fully implicit approach, in which the step size is often constrained by the nonlinear convergence anyway, we consider a method which allows the time step to vary spatially and satisfy a local CFL condition. In this way, we can increase the efficiency of the time stepping significantly in certain situations.

Another situation where local time stepping is useful is when modeling transport of some quantity by a highly varying velocity field. The advection of a species is described by an equation of the form

$$c_t + \nabla \cdot (\mathbf{u}c) = q, \tag{1}$$

where c is the concentration of the species, $\mathbf{u}$ is the velocity of the fluid transporting the species, and q represents source/sink terms. High resolution schemes have become popular for these problems, primarily because they are conservative and satisfy a maximum principle. The CFL constraint on the time step is determined by the ratio of the mesh spacing and the magnitude of the velocity. In certain cases, specifically in the presence of injection or production wells, the magnitude of $\mathbf{u}$ can vary substantially throughout the domain. In these situations, even if the mesh spacing is uniform, using a global CFL time step can be very restrictive, and local time stepping can result in substantial savings in computation time. It is important that the

*Received by the editors February 14, 2000; accepted for publication (in revised form) October 30, 2000; published electronically April 26, 2001. This work was supported by NSF grant DMS-9805491.
http://www.siam.org/journals/sisc/22-6/36773.html
†Center for Subsurface Modeling–C0200, Texas Institute for Computational and Applied Mathematics, University of Texas at Austin, Austin, TX 78712 (clint@ticam.utexas.edu, rob@ticam.utexas.edu).

local time stepping preserve the conservation and maximum principle properties of the underlying method. This situation was explored in some detail from a practical viewpoint in [3], and we will explore it from a more theoretical viewpoint here.

Local time stepping for one-dimensional scalar conservation laws was first proposed in Osher and Sanders [11]. They gave a thorough analysis of a first order spatial discretization with a local forward Euler time stepping scheme. This scheme allows each element to take either an entire time step or some fixed M smaller steps. In [3], the first author examined local time stepping for advection equations of the form (1), using high resolution schemes with slope limiters. Numerical results in two space dimensions were presented.

Another approach to local time stepping involves automatically taking smaller time steps where the mesh is refined. Berger and Oliger developed such an approach in [1], in which refined grids are laid over regions of the coarse mesh. These fine grids can have different orientation than the coarse one, and need not be nested. When the problem is integrated in time, small time steps are taken on the refined mesh and large time steps on the coarse mesh. Information is then passed between the grids by means of injection and interpolation. This approach allows higher order time integration, as the computation for each time step is done independently once the information is passed at the beginning of the time step.

In other work, Kallinderis and Baron [8] coupled the time refinement to the spatial refinement but used a single nonuniform mesh rather than multiple meshes. This work presented several methods (all first order) of handling the interface between regions with different time steps.

Flaherty et al. [5] have developed a parallel, adaptive discontinuous Galerkin method with a local forward Euler scheme which relies on interpolating values in time at interfaces between time steps of different sizes. This scheme, however, does not appear to conserve flux along these interfaces. Also, only first order in time methods are discussed.

In this paper, we seek to extend the work in [11] and [3] in two ways. First, we will show a maximum principle for a local forward Euler method when limited slopes are included. Second, we will show that the main ideas of local forward Euler discretizations may be extended to second order in time by way of the TVD Runge–Kutta methods of Gottlieb and Shu [6] and Shu [13]. A stability result for a constant coefficient case will be derived for this higher order method. We will also indicate how to extend this result to nonlinear problems. This analysis shows that we only need to satisfy a local CFL condition on each element.

The paper is outlined as follows. First, in section 2, we formulate a high resolution local forward Euler time discretization that employs some limited correction to the piecewise constant solution. In section 2.1, a maximum principle is derived for this approach. Then, a local time stepping procedure based on a second order time discretization is described in section 3, and a maximum principle for a simple case is given in section 3.1. Some extensions and implementation details are also discussed in this section. Finally, numerical results validating the theory are presented in section 4.

2. A high resolution method. We first consider the scalar conservation law

$$c_t + f(c)_x = 0, \tag{2}$$

together with the initial condition

$$c(x,0) = c_0(x). \tag{3}$$

We will partition the real line into intervals $I_j = \{x : x_{j-\frac{1}{2}} \le x < x_{j+\frac{1}{2}}\}$. We use the difference operator Δ_+ to denote a forward difference. That is, $\Delta_+ c_j \equiv c_{j+1} - c_j$ for some quantity c. A similar definition holds for Δ_- with $\Delta_- c_j \equiv c_j - c_{j-1}$. By integrating (2) over each I_j and using some consistent, Lipschitz numerical flux h at the cell edges, we obtain the semidiscrete scheme

$$\frac{dc_j}{dt} = -\frac{1}{\Delta x_j}\Delta_+ h(c_{j-1}, c_j), \tag{4}$$

where c_j is an approximation to the integral average of c over I_j. Examples of h include the Godunov flux and the Lax–Friedrichs flux. It is important that h is nondecreasing in the first variable and nonincreasing in the second variable. The initial condition is defined by simple projection. A standard forward Euler discretization can also be obtained in the obvious way.

In order to improve the accuracy of the above approach, we incorporate higher order "corrections" into the method. There are several ways of constructing these corrections. These include the piecewise linear reconstruction used in the monotone upwind scheme for conservation laws (MUSCL) of van Leer [14], the ENO reconstruction schemes of Harten and Osher [7], and the Runge–Kutta discontinuous Galerkin methods of Cockburn and Shu [2]. We shall not deal exclusively with any specific method but require certain properties of whichever is used. Since we are interested in second order accuracy, all of our examples assume linear approximations in space in each interval I_j.

After constructing the corrections and limiting them, we add them to the means to construct more accurate left and right states for the Riemann solutions. The corrections are denoted by tildes. Left states at an interface $x_{j+1/2}$ shall be denoted as $c_j + \tilde{c}_j \equiv c_{j+\frac{1}{2},L}$ and right states as $c_{j+1} - \tilde{\tilde{c}}_{j+1} \equiv c_{j+\frac{1}{2},R}$. In this way, the numerical flux at the edge is given by $h(c_{j+\frac{1}{2},L}, c_{j+\frac{1}{2},R})$.

Vital to the analysis is the assumption that the corrections introduce no new extrema into the solution. This allows corrections derived from the *minmod* slope limiter (described below) but rules out those derived from the modified *minmod* limiter of Shu [12] and the ENO schemes as introduced by Harten and Osher [7]. We can quantify this restriction as

$$-\theta \le \frac{\Delta_+ \tilde{\tilde{c}}_j}{\Delta_+ c_j} \le 1 \tag{5}$$

and

$$-\theta \le -\frac{\Delta_+ \tilde{c}_j}{\Delta_+ c_j} \le 1, \tag{6}$$

where $\theta \ge 0$.

The number θ is a chosen parameter which appears in the CFL condition. For example, see [2]. Geometrically, θ is related to the largest allowable ratio of differences between left and right states at consecutive edges relative to the means. This ratio can be allowed to be larger than 1, and we will see that such a situation will necessitate a restriction of the time step in order to guarantee a maximum principle. Consider the cells j and $j+1$ in Figure 1. The value $c_{j+\frac{1}{2},L} - c_{j-\frac{1}{2},L} \ge c_{j+1} - c_j$; however, the differences have the same sign. Thus

$$0 \le \frac{c_{j+\frac{1}{2},L} - c_{j-\frac{1}{2},L}}{c_{j+1} - c_j} = 1 + \frac{\Delta_+ \tilde{c}_j}{\Delta_+ c_j}, \tag{7}$$

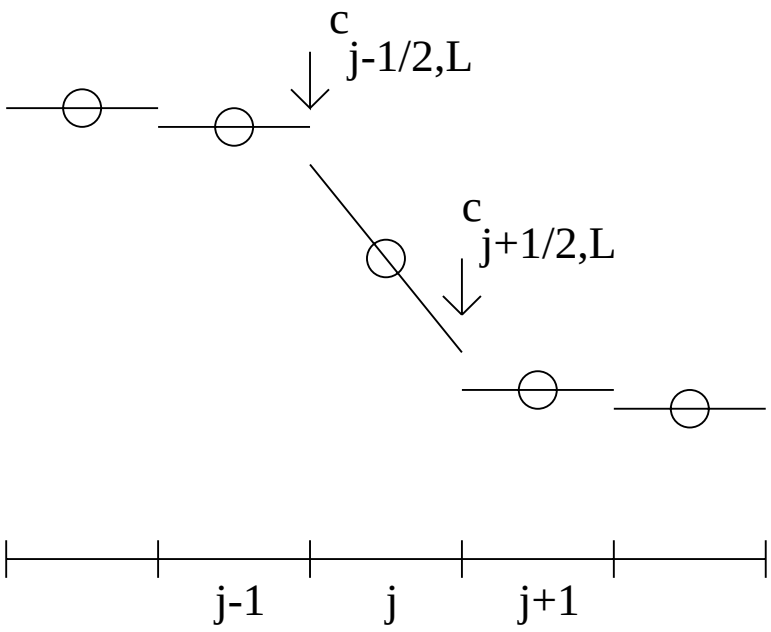

FIG. 1. *Slopes increase ratio of left states to means.*

and if θ satisfies (6), then

$$0 \leq \frac{c_{j+\frac{1}{2},L} - c_{j-\frac{1}{2},L}}{c_{j+1} - c_j} \leq 1 + \theta. \tag{8}$$

Specifically, suppose that we compute a slope, δc_j, using the *minmod* limiter. Thus,

$$\delta c_j = \begin{cases} \min\left(\frac{|\Delta_+ c_j|}{\Delta_+ x_j}, \frac{|\Delta_- c_j|}{\Delta_- x_j}\right) * \operatorname{sgn}(\Delta_+ c_j) & \text{if } \operatorname{sgn}(\Delta_+ c_j) = \operatorname{sgn}(\Delta_- c_j), \\ 0 & \text{otherwise.} \end{cases} \tag{9}$$

Set $\tilde{c}_j^u = \frac{\Delta x_j}{2} \delta c_j$. Then set

$$\tilde{c}_j = \begin{cases} \tilde{c}_j^u & \text{if } |\tilde{c}_j^u| \leq |\Delta_\pm c_j|, \\ 0 & \text{otherwise.} \end{cases} \tag{10}$$

This last limiting step is necessary only in the case of nonuniform mesh. Finally, $\tilde{\tilde{c}}_j = \tilde{c}_j$. The corrections then have the property that

$$\operatorname{sgn}\left(\frac{\tilde{c}_j}{\Delta_\pm c_j}\right) \geq 0. \tag{11}$$

We can thus make the bound

$$1 + \frac{\Delta_+ \tilde{c}_j}{\Delta_+ c_j} \leq 1 + \frac{\tilde{c}_{j+1}}{\Delta_+ c_j} \leq 2. \tag{12}$$

We also have

$$1 + \frac{\Delta_+ \tilde{c}_j}{\Delta_+ c_j} \geq 1 - \frac{\tilde{c}_j}{\Delta_+ c_j} \geq 0 \tag{13}$$

and

$$1 - \frac{\Delta_+ \tilde{\tilde{c}}_j}{\Delta_+ c_j} \geq 1 - \frac{\tilde{c}_{j+1}}{\Delta_+ c_j} \geq 0. \tag{14}$$

Hence, (5) and (6) hold automatically with the choice $\theta = 1$.

More generally, suppose corrections $\tilde{c}_j^u$ and $\tilde{\tilde{c}}_j^u$ are computed by some means, and θ is chosen such that $0 \leq \theta \leq 1$. Define

$$\tilde{c}_j = \begin{cases} \tilde{c}_j^u & \text{if } 2|\tilde{c}_j^u| \leq \theta |\Delta_\pm c_j|, \\ 0 & \text{otherwise,} \end{cases} \tag{15}$$

with an analogous definition for $\tilde{\tilde{c}}_j$. Then

$$1 + \frac{\Delta_+ \tilde{c}_j}{\Delta_+ c_j} \geq 1 - \frac{|\tilde{c}_{j+1}|}{|\Delta_+ c_j|} - \frac{|\tilde{c}_j|}{|\Delta_+ c_j|} \geq 1 - \theta \geq 0 \tag{16}$$

and

$$1 + \frac{\Delta_+ \tilde{c}_j}{\Delta_+ c_j} \leq 1 + \theta. \tag{17}$$

We now present the first order local time discretization. It is a straightforward extension of the method in [11]. The only difference is that the flux terms are computed using the corrected quantities $c_{j+1/2,L}$, $c_{j+1/2,R}$ rather than piecewise constants. We allow each element to take either a whole time step or some fixed M substeps per main time step.

We begin by noting that the intervals I_j form a partition of the real line. In addition to the spatial partition, we also introduce the temporal partition of $[0, T)$ into time intervals $[t^n, t^{n+1}), n = 0, \ldots, N-1$, with $t^0 = 0$ and $t^N = T$. We denote $\Delta t^n \equiv t^{n+1} - t^n$ and define $\lambda_j^n \equiv \frac{\Delta t^n}{\Delta x_j}$. In order to describe the local time stepping scheme, we will need to further partition the time steps on certain elements. We denote by $\mathcal{C}^n$ the set of all indices j such that a single time step is taken from t^n to t^{n+1} on I_j. On the rest of the elements, we partition the time step $[t^n, t^{n+1})$ into the union of substeps $[t^{n+\eta_l}, t^{n+\eta_{l+1}})$, $l = 0, \ldots, M-1$. Further, $\{\sigma_k\}_{k=1}^M$ is a sequence of positive numbers summing to unity. The numbers η_l are given as the cumulative sum of the σ_k, that is, $\eta_l = \sum_{k=1}^l \sigma_k$, and $\eta_0 = 0$. Correspondingly, the substeps in the time interval are given by $t^{n+\eta_{l+1}} = t^{n+\eta_l} + \sigma_{l+1} \Delta t^n$. Notice that the elements on which the local steps are taken may change over time.

With this notation established, we can modify the predictor-corrector scheme of Osher and Sanders to a so-called high resolution scheme in space.

Following [11], for each $k = 1, \ldots, M-1$, the "predictor" is defined by

$$c_j^{n+\eta_k} = \begin{cases} c_j^n, & j \in \mathcal{C}^n, \\ c_j^n - \lambda_j^n \sum_{l=0}^{k-1} \sigma_{l+1} \Delta_+ h(c_{j-1/2,L}^{n+\eta_l}, c_{j-1/2,R}^{n+\eta_l}), & j \notin \mathcal{C}^n, \end{cases} \tag{18}$$

and the "corrector" is

$$c_j^{n+1} = c_j^n - \lambda_j^n \sum_{l=0}^{M-1} \sigma_{l+1} \Delta_+ h(c_{j-\frac{1}{2},L}^{n+\eta_l}, c_{j-\frac{1}{2},R}^{n+\eta_l}). \tag{19}$$

Notice that if $j-1, j, j+1 \in \mathcal{C}^n$, then the method on I_j reduces to forward Euler with a step size of Δt^n.

2.1. A maximum principle. In this section, we present a maximum principle for the method (18)–(19). The maximum principle will verify that L^∞ stability is attainable with only local assumptions regarding the mesh, time step, velocity, and corrections. It is vital to this analysis that we use a "strict" limiter (i.e., one that does not introduce new extrema).

We introduce some notation for the scheme as follows. We define terms involving the differences of the corrections relative to the means:

$$\kappa_{j,1} \equiv 1 - \frac{\Delta_- \tilde{\tilde{c}}_j}{\Delta_- c_j} \tag{20}$$

and

$$\kappa_{j,2} \equiv 1 + \frac{\Delta_- \tilde{c}_j}{\Delta_- c_j}, \tag{21}$$

where we may have a superscript of n,$n+\eta_l$, etc. Note that (5) and (6) give us the bounds $0 \le \kappa_{j,1}, \kappa_{j,2} \le 1+\theta$. We also define the coefficients $\gamma_{j,1}$ and $\gamma_{j,2}$ as the local Lipschitz coefficients of h. That is,

$$\gamma_{j,1}^{n+\eta_l} \equiv -\Lambda_j^{n+\eta_l} \left[\frac{h\left(c_{j+\frac{1}{2},L}^{n+\eta_l}, c_{j+\frac{1}{2},R}^{n+\eta_l}\right) - h\left(c_{j+\frac{1}{2},L}^{n+\eta_l}, c_{j-\frac{1}{2},R}^{n+\eta_l}\right)}{c_{j+\frac{1}{2},R}^{n+\eta_l} - c_{j-\frac{1}{2},R}^{n+\eta_l}} \right] \tag{22}$$

and

$$\gamma_{j,2}^{n+\eta_l} \equiv -\Lambda_j^{n+\eta_l} \left[\frac{h\left(c_{j+\frac{1}{2},L}^{n+\eta_l}, c_{j-\frac{1}{2},R}^{n+\eta_l}\right) - h\left(c_{j-\frac{1}{2},L}^{n+\eta_l}, c_{j-\frac{1}{2},R}^{n+\eta_l}\right)}{c_{j+\frac{1}{2},L}^{n+\eta_l} - c_{j-\frac{1}{2},L}^{n+\eta_l}} \right], \tag{23}$$

where

$$\Lambda_j^{n+\eta_l} = \begin{cases} \lambda_j^n & \text{if } j-1, j \text{ or } j+1 \in \mathcal{C}^n, \\ \sigma_{l+1}\lambda_j^n & \text{otherwise.} \end{cases} \tag{24}$$

If the flux f is smooth enough, then we can, as in [11], reduce the Lipschitz constants to a local supremum of $f'(c)$. Further, we define the terms

$$\alpha_{j,1} \equiv \gamma_{j,1}\kappa_{j,1} \tag{25}$$

and

$$\alpha_{j,2} \equiv \gamma_{j,2}\kappa_{j,2}. \tag{26}$$

By our assumptions (5) and (6) and the assumed monotonicity properties of h (h nondecreasing in its first argument, nonincreasing in its second), we have $\alpha_{j,1} \ge 0$, $\alpha_{j,2} \le 0$, and thus

$$\alpha_{j,1} - \alpha_{j,2} \ge 0. \tag{27}$$

For each j at each time $t^{n+\eta_l}$, we require the local CFL condition

$$1 - \alpha_{j,1}^{n+\eta_l} + \alpha_{j,2}^{n+\eta_l} \ge 0. \tag{28}$$

Here, we pause to discuss the relation between the terms (5)–(6) and the CFL condition (28). We require that

$$\alpha_{j,1}^{n+\eta_l} - \alpha_{j,2}^{n+\eta_l} \leq 1, \tag{29}$$

or

$$\gamma_{j,1}^{n+\eta_l} \kappa_{j,1}^{n+\eta_l} - \gamma_{j,2}^{n+\eta_l} \kappa_{j,2}^{n+\eta_l} \leq 1. \tag{30}$$

If the corrections are all zero, then each κ term is simply 1. However, as in Figure 1, our κ terms are only bounded by $1+\theta$. Consequently, in order to satisfy (28), we must possibly take a smaller time step than we would if we were not using the corrections. Equivalently, we could write our CFL condition as do Cockburn and Shu [2]:

$$\gamma_{j,1}^{n+\eta_l} - \gamma_{j,2}^{n+\eta_l} \leq \frac{1}{1+\theta}. \tag{31}$$

The L^∞ stability result of [11] depends upon showing that the operator which advances the solution forward is monotone. However, with the addition of the correction terms, the operator ceases to be monotone, and we must take a different approach. We begin by examining the basic global time stepping method (or $j \in \mathcal{C}^n \ \forall \ j$). The method is

$$c_j^{n+1} = c_j^n - \lambda_j^n \left[h\left(c_{j+\frac{1}{2},L}^n, c_{j+\frac{1}{2},R}^n \right) - h\left(c_{j-\frac{1}{2},L}^n, c_{j-\frac{1}{2},R}^n \right) \right]. \tag{32}$$

We can obtain L^∞ stability as follows. Add and subtract $h(c_{j+\frac{1}{2},L}^n, c_{j-\frac{1}{2},R}^n)$ in (32) and multiply and divide by the proper differences, and we have

$$c_j^{n+1} = c_j^n + \alpha_{j,1}^n \left(c_{j+1}^n - c_j^n \right) + \alpha_{j,2}^n \left(c_j^n - c_{j-1}^n \right), \tag{33}$$

or

$$c_j^{n+1} = \left(1 - \alpha_{j,1}^n + \alpha_{j,2}^n \right) c_j^n + \alpha_{j,1}^n c_{j+1}^n - \alpha_{j,2}^n c_{j-1}^n. \tag{34}$$

Then, by (27) and (28), we see that

$$\begin{aligned} |c_j^{n+1}| &\leq \left(1 - \alpha_{j,1}^n + \alpha_{j,2}^n \right) |c_j^n| + \alpha_{j,1}^n |c_{j+1}^n| - \alpha_{j,2}^n |c_{j-1}^n| \\ &\leq \sup_j |c_j^n|. \end{aligned} \tag{35}$$

By making similar arguments in the context of the local time stepping method, we have the following stability result.

PROPOSITION 2.1. *Assume* (5), (6), *and* (28) *hold, and the numerical flux* $h(u,v)$ *is nondecreasing in* u *and nonincreasing in* v*; then for* $n > 0$,

$$\sup_j |c_j^n| \leq \sup_j |c_j^0|,$$

where c_j^n *is defined by* (18)–(19).

Proof. The proof follows from looking separately at the cases in which $j \in \mathcal{C}^n$ and $j \notin \mathcal{C}^n$.

We begin with the case of $j \notin \mathcal{C}^n$. In this case, we may use the same technique as in the global time stepping case recursively to bound the solution at time $n+1$ in terms of the solution at time n.

$$
\begin{aligned}
|c_j^{n+\eta_l}| &= \left| c_j^{n+\eta_{l-1}} - \sigma_{l+1}\lambda_j^n \Delta_+ h\left(c_{j-\frac{1}{2},L}^{n+\eta_{l-1}}, c_{j-\frac{1}{2},R}^{n+\eta_{l-1}}\right)\right| \\
&= \left| c_j^{n+\eta_{l-1}} + \alpha_{j,1}^{n+\eta_{l-1}}\left(c_{j+1}^{n+\eta_{l-1}} - c_j^{n+\eta_{l-1}}\right)\right. \\
&\quad \left. + \alpha_{j,2}^{n+\eta_{l-1}}\left(c_j^{n+\eta_{l-1}} - c_{j-1}^{n+\eta_{l-1}}\right)\right| \\
&= |c_j^{n+\eta_{l-1}}|\left(1 - \alpha_{j,1}^{n+\eta_{l-1}} + \alpha_{j,2}^{n+\eta_{l-1}}\right) \\
&\quad + \alpha_{j,1}^{n+\eta_{l-1}}|c_{j+1}^{n+\eta_{l-1}}| - \alpha_{j,2}^{n+\eta_{l-1}}|c_{j-1}^{n+\eta_{l-1}}| \\
&\leq \max_{j-1\leq k\leq j+1} |c_k^{n+\eta_{l-1}}|.
\end{aligned} \tag{36}
$$

The α terms satisfy the same sign conditions as their global time stepping counterparts, so

$$
|c_j^{n+\eta_l}| \leq \max_{j-1\leq k\leq j+1} |c_k^{n+\eta_{l-1}}|. \tag{37}
$$

If $j^* \in [j-1, j+1]$ is the element on which the maximum occurs, and if $j^* \in \mathcal{C}^n$, then we are done for this element, as we have the solution bounded in terms of values at time n. If $j^* \notin \mathcal{C}^n$, then we apply this argument recursively.

Now, suppose that $j \in \mathcal{C}^n$. Using (18) in (19),

$$
\begin{aligned}
c_j^{n+1} &= c_j^n - \lambda_j^n \sum_{l=0}^{M-1} \sigma_{l+1}\Delta_+ h\left(c_{j-\frac{1}{2},L}^{n+\eta_l}, c_{j-\frac{1}{2},R}^{n+\eta_l}\right) \\
&= \sum_{l=0}^{M-1} \sigma_{l+1}\left(c_j^{n+\eta_{l-1}} - \lambda_j^n \Delta_+ h\left(c_{j-\frac{1}{2},L}^{n+\eta_l}, c_{j-\frac{1}{2},R}^{n+\eta_l}\right)\right) \\
&= \sum_{l=0}^{M-1} \sigma_{l+1}\left[c_j^{n+\eta_{l-1}} + \alpha_{j,1}^{n+\eta_{l-1}}\left(c_{j+1}^{n+\eta_{l-1}} - c_j^{n+\eta_{l-1}}\right)\right. \\
&\quad \left. + \alpha_{j,2}^{n+\eta_{l-1}}\left(c_j^{n+\eta_{l-1}} - c_{j-1}^{n+\eta_{l-1}}\right)\right] \\
&= \sum_{l=0}^{M-1} \sigma_{l+1}\left[c_j^{n+\eta_{l-1}}\left(1 - \alpha_{j,1}^{n+\eta_{l-1}} + \alpha_{j,2}^{n+\eta_{l-1}}\right)\right. \\
&\quad \left. + \alpha_{j,1}^{n+\eta_{l-1}} c_{j+1}^{n+\eta_{l-1}} - \alpha_{j,2}^{n+\eta_{l-1}} c_{j-1}^{n+\eta_{l-1}}\right].
\end{aligned} \tag{38}
$$

Again, using the monotonicity of h and (28), we have the sign conditions for the α terms, and

$$
\begin{aligned}
|c_j^{n+1}| &\leq \sum_{l=0}^{M-1} \sigma_{l+1}\left[|c_j^{n+\eta_{l-1}}|\left(1 - \alpha_{j,1}^{n+\eta_{l-1}} + \alpha_{j,2}^{n+\eta_{l-1}}\right)\right. \\
&\quad \left. + \alpha_{j,1}^{n+\eta_{l-1}}|c_{j+1}^{n+\eta_{l-1}}| - \alpha_{j,2}^{n+\eta_{l-1}}|c_{j-1}^{n+\eta_{l-1}}|\right] \\
&\leq \sum_{l=0}^{M-1} \sigma_{l+1} \max_{j-1\leq k\leq j+1} |c_k^{n+\eta_{l-1}}|.
\end{aligned} \tag{39}
$$

Now, each term $|c_k^{n+\eta_{l-1}}|$ may be bounded by prior information. If $k \in \mathcal{C}^n$, then $c_k^{n+\eta_{l-1}} = c_k^n$ and the bound is obvious. Otherwise, the above bound for $j \notin \mathcal{C}^n$ applies, and we are done. ∎

Note that while c_j^n remains constant in time on I_j, we might have to modify the correction terms on I_j at intermediate times if $j \in \mathcal{C}^n$ and $j-1 \notin \mathcal{C}^n$ or $j+1 \notin \mathcal{C}^n$ to avoid adding extrema to the solution.

Note also that for general problems, the CFL condition (28) for substeps after the first when $j \notin \mathcal{C}^n$ cannot be verified a priori without adjusting the time step at each substep. However, examining (25) and (26), we have uniform bounds on the κ terms by doing appropriate limiting. Moreover, with some knowledge of f, we can bound the γ terms locally depending on $f'(c)$ and the local mesh spacing. Thus we can estimate an upper bound on the α terms over regions of the domain, which can be used to set the local time steps over these regions. We have used this approach successfully in practice.

3. A second order time stepping scheme. We now turn to developing a local time stepping procedure based on a formally second order method. We are again interested in integrating the semidiscrete scheme

$$\frac{dc_j}{dt} = -\frac{1}{\Delta x_j}\Delta_+ h(c_{j-1/2,L}, c_{j-1/2,R}). \tag{40}$$

We first describe the basic method we are using, which is a second order Runge–Kutta scheme (in particular, Heun's method), shown to be TVD in [13, 6]. Then, we formulate the scheme for handling the interface between two regions with different time steps. We will assume the basic method holds for some distance away from the interfaces.

Heun's method for integrating (40) is given by

$$\overline{c}_j^{n+1} = c_j^n - \lambda_j^n \Delta_+ h(c_{j-1/2,L}^n, c_{j-1/2,R}^n), \tag{41}$$

$$w_j^{n+1} = \overline{c}_j^{n+1} - \lambda_j^n \Delta_+ h(\overline{c}_{j-1/2,L}^{n+1}, \overline{c}_{j-1/2,R}^{n+1}), \tag{42}$$

$$c_j^{n+1} = \frac{1}{2}\left(c_j^n + w_j^{n+1}\right). \tag{43}$$

Here $\overline{c}_{j+1/2,L}^{n+1} = \overline{c}_j^{n+1} + \tilde{\overline{c}}_j^{n+1}$, with an analogous definition for $\overline{c}_{j+1/2,R}^{n+1}$, where the corrections are computed as in (5)–(6). This method is nothing more than a convex combination of forward Euler steps and the initial value. Correspondingly, using the properties of the forward Euler method analyzed in the previous section, one easily obtains stability for this scheme.

PROPOSITION 3.1. *For the scheme* (41)–(43), *with corrections limited as in* (5)–(6) *and a CFL time-step constraint as in* (28), *we have*

$$\sup_j |c_j^n| \le \sup_j |c_j^0|.$$

For now, we are interested in computing at the interface on the space-time mesh shown in Figure 2. Thus, the time step in interval I_{j+1} is Δt and in I_j, $\Delta t/2$. For

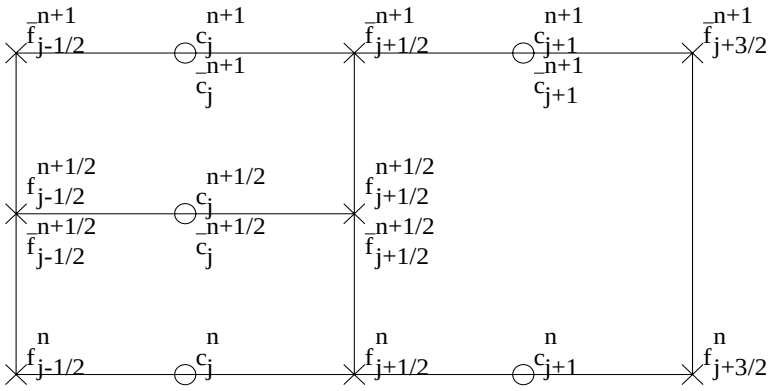

FIG. 2. *Local time stepping mesh.*

simplicity, we assume the time step is Δt for intervals to the right of $x_{j+1/2}$ and $\Delta t/2$ for intervals to the left of $x_{j+1/2}$. We will also assume for simplicity that $f(c) = uc$, where $u > 0$. We will describe the method and state conditions which the corrections $\tilde{c}$ should satisfy to ensure a maximum principle. We will then describe in more detail how the corrections may be constructed so as to satisfy these conditions. Finally, we will describe the method when the situation in Figure 2 holds and $u < 0$, and then discuss generalizations to a nonlinear flux function and to the case with M steps.

Thus, assuming $f(c) = uc$, where $u > 0$, to compute the solution in elements I_j and I_{j+1}, we use the following procedure.

Scheme I ($u > 0$).

(i) Compute corrections $\tilde{c}^n_{j-1}$, $\tilde{c}^n_j$, and $\tilde{c}^{n,1}_{j+1}$ by some means and limit them so that (44) is satisfied.

(ii) $\bar{c}^{n+\frac{1}{2}}_j = c^n_j - \frac{u\lambda^n_j}{2}\left[c^n_j + \tilde{c}^n_j - \left(c^n_{j-1} + \tilde{c}^n_{j-1}\right)\right]$.

(iii) Compute $\tilde{\bar{c}}^{n+1/2}_{j-1}$, $\tilde{\bar{c}}^{n+1/2}_j$, and $\tilde{c}^{n,2}_{j+1}$ so that (45) is satisfied.

(iv) $w^{n+\frac{1}{2}}_j = \bar{c}^{n+\frac{1}{2}}_j - \frac{u\lambda^n_j}{2}[\bar{c}^{n+\frac{1}{2}}_j + \tilde{\bar{c}}^{n+\frac{1}{2}}_j - (\bar{c}^{n+\frac{1}{2}}_{j-1} + \tilde{\bar{c}}^{n+\frac{1}{2}}_{j-1})]$.

(v) $c^{n+\frac{1}{2}}_j = \frac{1}{2}(c^n_j + w^{n+\frac{1}{2}}_j)$.

(vi) Define $\tilde{c}^n_{j+1} \equiv \frac{1}{2}(\tilde{c}^{n,1}_{j+1} + \tilde{c}^{n,2}_{j+1})$.

(vii) $\bar{c}^{n+1}_{j+1} = c^{n+1/2}_{j+1} - u\lambda^n_{j+1}[c^n_{j+1} + \tilde{c}^n_{j+1} - \frac{1}{2}(c^n_j + \tilde{c}^n_j + \bar{c}^{n+\frac{1}{2}}_j + \tilde{\bar{c}}^{n+\frac{1}{2}}_j)]$.

(viii) Compute $\tilde{c}^{n+\frac{1}{2}}_{j-1}$, $\tilde{c}^{n+\frac{1}{2}}_j$, and $\tilde{\bar{c}}^{n+1,1}_{j+1}$ so that (46) is satisfied.

(iv) $\bar{c}^{n+1}_j = c^n_j - \frac{u\lambda^n_j}{2}[c^{n+\frac{1}{2}}_j + \tilde{c}^{n+\frac{1}{2}}_j - (c^{n+\frac{1}{2}}_{j-1} + \tilde{c}^{n+\frac{1}{2}}_{j-1})]$.

(x) Compute $\tilde{\bar{c}}^{n+1}_{j-1}$, $\tilde{\bar{c}}^{n+1}_j$, and $\tilde{\bar{c}}^{n+1,2}_{j+1}$ so that (47) is satisfied.

(xi) $w^{n+1}_j = \bar{c}^{n+1}_j - \frac{u\lambda^n_j}{2}[\bar{c}^{n+1}_j + \tilde{\bar{c}}^{n+1}_j - (\bar{c}^{n+1}_{j-1} + \tilde{\bar{c}}^{n+1}_{j-1})]$.

(xii) $c^{n+1}_j = \frac{1}{2}(c^{n+\frac{1}{2}}_j + w^{n+1}_j)$.

(xiii) Define $\tilde{\bar{c}}^{n+1}_{j+1} \equiv \frac{1}{2}(\tilde{\bar{c}}^{n,1}_{j+1} + \tilde{\bar{c}}^{n,2}_{j+1})$.

(xiv) $w^{n+1}_{j+1} = \bar{c}^n_{j+1} - u\lambda^n_{j+1}[\bar{c}^n_{j+1} + \tilde{\bar{c}}^n_{j+1} - \frac{1}{2}(c^{n+\frac{1}{2}}_j + \tilde{c}^{n+\frac{1}{2}}_j + \bar{c}^{n+1}_j + \tilde{\bar{c}}^{n+1}_j)]$.

(xv) $c^{n+1}_{j+1} = \frac{1}{2}\left(c^n_{j+1} + w^{n+1}_{j+1}\right)$.

The corrections should satisfy the following conditions to guarantee a maximum principle:

$$-\theta \le -\frac{\tilde{c}_j^n - \tilde{c}_{j-1}^n}{c_j^n - c_{j-1}^n},\ -\frac{\tilde{c}_{j+1}^{n,1} - \tilde{c}_j^n}{c_{j+1}^n - c_j^n} \le 1, \tag{44}$$

$$-\theta \le -\frac{\tilde{\bar{c}}_j^{n+\frac{1}{2}} - \tilde{\bar{c}}_{j-1}^{n+\frac{1}{2}}}{\bar{c}_j^{n+\frac{1}{2}} - \bar{c}_{j-1}^{n+\frac{1}{2}}},\ -\frac{\tilde{c}_{j+1}^{n,2} - \tilde{\bar{c}}_j^{n+\frac{1}{2}}}{c_{j+1}^n - \bar{c}_j^{n+\frac{1}{2}}} \le 1, \tag{45}$$

$$-\theta \le -\frac{\tilde{\bar{c}}_j^{n+\frac{1}{2}} - \tilde{c}_{j-1}^{n+\frac{1}{2}}}{c_j^{n+\frac{1}{2}} - c_{j-1}^{n+\frac{1}{2}}},\ -\frac{\tilde{\bar{c}}_{j+1}^{n+1,1} - \tilde{\bar{c}}_j^{n+\frac{1}{2}}}{\bar{c}_{j+1}^{n+1} - c_j^{n+1/2}} \le 1, \tag{46}$$

$$-\theta \le -\frac{\tilde{\bar{c}}_j^{n+1} - \tilde{\bar{c}}_{j-1}^{n+1}}{\bar{c}_j^{n+1} - \bar{c}_{j-1}^{n+1}},\ -\frac{\tilde{\bar{c}}_{j+1}^{n+1,2} - \tilde{\bar{c}}_j^{n+1}}{\bar{c}_{j+1}^{n+1} - \bar{c}_j^{n+1}} \le 1. \tag{47}$$

3.1. A maximum principle for the second order method. In this section, we derive a maximum principle for Scheme I above. The maximum principle argument allows for the method to have a time step on one cell that would violate the CFL condition on the adjacent cell. In particular, we assume

$$\frac{u\Delta t^n}{2\Delta x_j} \le \frac{1}{1+\theta} \tag{48}$$

and

$$\frac{u\Delta t^n}{\Delta x_{j+1}} \le \frac{1}{1+\theta}, \tag{49}$$

which is the usual CFL condition for grid blocks I_j and I_{j+1}.

Away from the interface, where the time step among adjacent cells is the same, the stability of the method is easily demonstrated. We summarize the result in the following proposition.

PROPOSITION 3.2. *Assume a time step of size Δt^n for all elements to the right of $x_{j+1/2}$ and size $\Delta t^n/2$ for all elements to the left of $x_{j+1/2}$, where Δt^n satisfies* (48) *and* (49). *Then, for Scheme* I *above with $f(c) = uc$ where $u > 0$, with corrections satisfying* (44)–(47) *on I_j and I_{j+1} and* (5)–(6) *elsewhere, we have*

$$\sup_j |c_j^n| \le \sup_j |c_j^0|. \tag{50}$$

Proof. For all blocks except I_j and I_{j+1}, the bound $|c_i^{n+1}| \le \sup_j |c_j^n|$ follows from the arguments used to prove Propositions 2.1 and 3.1. Furthermore, the only difference between the computation on I_j and the standard method is that there are somewhat different restrictions on the corrections, namely, they should satisfy (44)–(47). Thus, one can easily show that $|\bar{c}_j^{n+\frac{1}{2}}|$, $|w_j^{n+\frac{1}{2}}|$, $|c_j^{n+\frac{1}{2}}|$, $|\bar{c}_j^{n+1}|$, $|w_j^{n+1}|$ and hence $|c_j^{n+1}|$ are all bounded above by $\sup_j |c_j^n|$.

The solution on I_{j+1} must be more carefully analyzed. We will first show a maximum principle for $|\overline{c}_{j+1}^{n+1}|$. Then, this will be used to show maximum principles for $|w_{j+1}^{n+1}|$ and $|c_{j+1}^{n+1}|$.

Consider $\overline{c}_{j+1}^{n+1}$. The argument will proceed by the standard technique of choosing the CFL condition and using the restrictions on the corrections to guarantee that $\overline{c}_{j+1}^{n+1}$ is a convex combination of previous values. We define

$$\kappa_1 = 1 + \frac{\tilde{c}_{j+1}^{n,1} - \tilde{c}_j^n}{c_{j+1}^n - c_j^n} \tag{51}$$

and

$$\kappa_2 = 1 + \frac{\tilde{c}_{j+1}^{n,2} - \tilde{\overline{c}}_j^{n+\frac{1}{2}}}{c_{j+1}^n - \overline{c}_j^{n+\frac{1}{2}}}. \tag{52}$$

We can write the computation of $\overline{c}_{j+1}^n$ as

(53)

$$\begin{aligned}
\overline{c}_{j+1}^{n+1} &= c_{j+1}^n - \frac{u\Delta t^n}{\Delta x_{j+1}} \left[\left(c_{j+1}^n + \tilde{c}_{j+1}^n \right) - \frac{1}{2} \left(\left(c_j^n + \tilde{c}_j^n \right) - \left(\overline{c}_j^{n+\frac{1}{2}} + \tilde{\overline{c}}_j^{n+\frac{1}{2}} \right) \right) \right] \\
&= c_{j+1}^n - \frac{u\Delta t^n}{2\Delta x_{j+1}} \left[c_{j+1}^n + \tilde{c}_{j+1}^{n,1} - \left(c_j^n + \tilde{c}_j^n \right) + c_{j+1}^n + \tilde{c}_{j+1}^{n,2} - \left(\overline{c}_j^{n+\frac{1}{2}} + \tilde{\overline{c}}_j^{n+\frac{1}{2}} \right) \right] \\
&= c_{j+1}^n - \frac{u\Delta t^n}{2\Delta x_{j+1}} \left[\kappa_1 \left(c_{j+1}^n - c_j^n \right) + \kappa_2 \left(c_{j+1}^n - \overline{c}_j^{n+\frac{1}{2}} \right) \right] \\
&= c_{j+1}^n \left[1 - \frac{u\Delta t^n}{2\Delta x_{j+1}} \left(\kappa_1 + \kappa_2 \right) \right] + \frac{u\Delta t^n}{2\Delta x_{j+1}} \kappa_1 c_j^n + \frac{u\Delta t^n}{2\Delta x_{j+1}} \kappa_2 \overline{c}_j^{n+\frac{1}{2}}.
\end{aligned}$$

We note that the coefficients of the terms sum to 1. By (44) and (45), $\kappa_i \geq 0$, $i = 1, 2$, and

$$1 - \frac{u\Delta t^n}{2\Delta x_{j+1}} \left(\kappa_1 + \kappa_2 \right) \geq 0 \tag{54}$$

if the time step is chosen such that (49) is satisfied.

By the above-stated bound on $|\overline{c}_j^{n+\frac{1}{2}}|$, we can take the absolute value of each side of (53) and obtain

$$\begin{aligned}
|\overline{c}_{j+1}^{n+1}| &= |c_{j+1}^n| \left[1 - \frac{u\Delta t^n}{2\Delta x_{j+1}} \left(\kappa_1 + \kappa_2 \right) \right] + \frac{u\Delta t^n}{2\Delta x_{j+1}} \kappa_1 |c_j^n| + \frac{u\Delta t^n}{2\Delta x_{j+1}} \kappa_2 |\overline{c}_j^{n+\frac{1}{2}}| \\
&\leq \sup_j |c_j^n|.
\end{aligned} \tag{55}$$

Next, consider w_{j+1}^{n+1}. We define two new terms:

$$\kappa_3 = 1 + \frac{\tilde{\overline{c}}_{j+1}^{n+1,2} - \tilde{c}_j^{n+\frac{1}{2}}}{\overline{c}_{j+1}^{n+1} - c_j^{n+\frac{1}{2}}} \tag{56}$$

and

$$\kappa_4 = 1 + \frac{\tilde{\overline{c}}_{j+1}^{n+1,1} - \tilde{\overline{c}}_j^{n+1}}{\overline{c}_{j+1}^{n+1} - \overline{c}_j^{n+1}}. \tag{57}$$

The method can be written as

$$
\begin{aligned}
w_{j+1}^{n+1} &= \overline{c}_{j+1}^{n+1} - \frac{u\Delta t^n}{\Delta x_{j+1}}\left[\overline{c}_{j+1}^{n+1} + \tilde{\overline{c}}_{j+1}^{n+1} - \frac{1}{2}\left(c_j^{n+\frac{1}{2}} + \tilde{c}_j^{n+\frac{1}{2}} + \overline{c}_j^{n+1} + \tilde{\overline{c}}_j^{n+1}\right)\right] \\
&= \overline{c}_{j+1}^{n+1} - \frac{u\Delta t^n}{2\Delta x_{j+1}}\left[\overline{c}_{j+1}^{n+1} + \tilde{\overline{c}}_{j+1}^{n+1,1}\right. \\
&\qquad \left. - \left(c_j^{n+\frac{1}{2}} + \tilde{c}_j^{n+\frac{1}{2}}\right) + \overline{c}_{j+1}^{n+1} + \tilde{\overline{c}}_{j+1}^{n+1,2} - \left(\overline{c}_j^{n+1} + \tilde{\overline{c}}_j^{n+1}\right)\right] \\
&= \overline{c}_{j+1}^{n+1} - \frac{u\Delta t}{2\Delta x_{j+1}}\left[\kappa_3\left(\overline{c}_{j+1}^{n+1} - c_j^{n+\frac{1}{2}}\right) + \kappa_4\left(\overline{c}_{j+1}^{n+1} - \overline{c}_j^{n+1}\right)\right] \\
&= \overline{c}_{j+1}^{n+1}\left[1 - \frac{u\Delta t^n}{2\Delta x_{j+1}}\left(\kappa_3 + \kappa_4\right)\right] + \frac{u\Delta t^n}{2\Delta x_{j+1}}\kappa_3 c_j^{n+\frac{1}{2}} + \frac{u\Delta t^n}{2\Delta x_{j+1}}\kappa_4 \overline{c}_j^{n+1}.
\end{aligned} \tag{58}
$$

As before, the coefficients sum to 1. By a similar argument, (46) and (47) give the nonnegativity of each κ term, and we have the same CFL restriction (49) as above. Taking the absolute value of each side of (58), we see that

$$
|w_{j+1}^{n+1}| \le \max\left(|\overline{c}_{j+1}^{n+1}|, |c_j^{n+\frac{1}{2}}|, |\overline{c}_j^{n+1}|\right),
$$

and each of these terms is bounded by the solution at time n. Finally

$$
\begin{aligned}
|c_{j+1}^{n+1}| &= \left|\frac{1}{2}\left(c_{j+1}^n + w_{j+1}^{n+1}\right)\right| \\
&\le \frac{1}{2}|c_{j+1}^n| + \frac{1}{2}|w_{j+1}^{n+1}| \\
&\le \sup_j |c_j^n|. \qquad \square
\end{aligned}
$$

To summarize, our method is conservative (the flux used at the right edge of element I_j is equal to that used at the left edge of I_{j+1}). We have demonstrated stability subject only to local CFL restrictions. Next we discuss the limiting of the corrections so that the conditions (44)–(47) are satisfied. Later, we will present numerical evidence demonstrating that local time stepping does not appear to degrade the accuracy of the method.

3.2. Computing and limiting the corrections. We discuss in slightly more detail the computation of the $\tilde{c}$ terms. We assume as before that θ is chosen so that $0 \le \theta \le 1$.

First, assume $\tilde{c}_j^n$, $\tilde{c}_{j-1}^n$, and $\tilde{c}_{j+1}^{n,1}$ are computed so that (44) is satisfied, say, using (15). We then set

$$
\tilde{c}_{j+1}^{n,2} = \begin{cases} \tilde{c}_{j+1}^{n,1} & \text{if } 2|\tilde{c}_{j+1}^{n,1}| \le \theta|c_{j+1}^n - \overline{c}_j^{n+1/2}|, \\ 0 & \text{otherwise.} \end{cases} \tag{59}
$$

In a similar way, corrections $\tilde{\overline{c}}_j^{n+1/2}$ and $\tilde{\overline{c}}_{j-1}^{n+1/2}$ are computed so that the first inequality in (45) is satisfied, and $\tilde{\overline{c}}_j^{n+1/2}$ is limited so that

$$
2|\tilde{\overline{c}}_j^{n+1/2}| \le \theta|c_{j+1}^n - \overline{c}_j^{n+1/2}|. \tag{60}
$$

Hence, one can show

$$
0 \le \kappa_1, \kappa_2 \le 1 + \theta. \tag{61}
$$

Proceeding, $\tilde{c}_j^{n+1/2}$ and $\tilde{c}_{j-1}^{n+1/2}$ are computed so that the first inequality in (46) is satisfied, and so that

$$2|\tilde{c}_j^{n+1/2}| \le \theta|\overline{c}_{j+1}^{n+1} - c_j^{n+1/2}|; \tag{62}$$

$\tilde{\overline{c}}_{j+1}^{n+1,1}$ is computed so that it also satisfies

$$2|\tilde{c}_{j+1}^{n+1,1}| \le \theta|\overline{c}_{j+1}^{n+1} - c_j^{n+1/2}|. \tag{63}$$

Similarly, $\tilde{\overline{c}}_{j-1}^{n+1}$, $\tilde{\overline{c}}_j^{n+1}$, and $\tilde{\overline{c}}_{j+1}^{n+1,2}$ are computed so that (47) is satisfied. Thus

$$0 \le \kappa_3, \kappa_4 \le 1 + \theta. \tag{64}$$

3.3. The case $u < 0$. Consider Figure 2 again, now with $f(c) = uc$ and $u < 0$. This case is analogous to the situation in which $u > 0$ and the picture in Figure 2 is reversed, namely, the local time steps are to the right of the interface. In this case, to compute the solution in elements I_j and I_{j+1}, we use the following procedure.

Scheme II ($u < 0$).

(i) Compute corrections $\tilde{c}_j^n$, $\tilde{c}_{j+1}^{n,1}$, and $\tilde{c}_{j+2}^n$ so that (65) is satisfied.

(ii) $\overline{c}_j^{n+\frac{1}{2}} = c_j^n - \frac{u\lambda_j^n}{2}[c_{j+1}^n - \tilde{c}_{j+1}^{n,1} - (c_j^n - \tilde{c}_j^n)]$.

(iii) Compute $\tilde{\overline{c}}_j^{n+1/2}$ and $\tilde{c}_{j+1}^{n,2}$ so that (66) is satisfied.

(iv) $w_j^{n+\frac{1}{2}} = \overline{c}_j^{n+\frac{1}{2}} - \frac{u\lambda_j^n}{2}[c_{j+1}^n - \tilde{c}_{j+1}^{n,2} - (\overline{c}_j^{n+\frac{1}{2}} - \tilde{\overline{c}}_j^{n+\frac{1}{2}})]$.

(v) $c_j^{n+\frac{1}{2}} = \frac{1}{2}(c_j^n + w_j^{n+\frac{1}{2}})$.

(vi) Define $\tilde{c}_{j+1}^n \equiv \frac{1}{2}(\tilde{c}_{j+1}^{n,1} + \tilde{c}_{j+1}^{n,2})$.

(vii) $\overline{c}_{j+1}^{n+1} = c_{j+1}^n - u\lambda_{j+1}^n\left[c_{j+2}^n - \tilde{c}_{j+2}^n - \left(c_{j+1}^n - \tilde{c}_{j+1}^n\right)\right]$.

(viii) Compute $\tilde{c}_j^{n+\frac{1}{2}}$, $\tilde{\overline{c}}_{j+1}^{n+1,1}$, and $\tilde{\overline{c}}_{j+2}^{n+1}$ so that (67) is satisfied.

(ix) $\overline{c}_j^{n+1} = c_j^{n+1/2} - \frac{u\lambda_j^n}{2}[\overline{c}_{j+1}^{n+1} - \tilde{\overline{c}}_{j+1}^{n+1,1} - (c_j^{n+\frac{1}{2}} - \tilde{c}_j^{n+\frac{1}{2}})]$.

(x) Compute $\tilde{\overline{c}}_j^{n+1}$ and $\tilde{\overline{c}}_{j+1}^{n+1,2}$ to satisfy (68).

(xi) $w_j^{n+1} = \overline{c}_j^{n+1} - \frac{u\lambda_j^n}{2}[\overline{c}_{j+1}^{n+1} - \tilde{\overline{c}}_{j+1}^{n+1,2} - (\overline{c}_j^{n+1} - \tilde{\overline{c}}_j^{n+1})]$.

(xii) $c_j^{n+1} = \frac{1}{2}(c_j^{n+\frac{1}{2}} + w_j^{n+1})$.

(xiii) Define $\tilde{\overline{c}}_{j+1}^{n+1} \equiv \frac{1}{2}(\tilde{\overline{c}}_{j+1}^{n+1,1} + \tilde{\overline{c}}_{j+1}^{n+1,2})$.

(xiv) $w_{j+1}^{n+1} = \overline{c}_{j+1}^n - u\lambda_{j+1}^n[\overline{c}_{j+2}^{n+1} - \tilde{\overline{c}}_{j+2}^{n+1} - (\overline{c}_{j+1}^{n+1} - \tilde{\overline{c}}_j^{n+1})]$.

(xv) $c_{j+1}^{n+1} = \frac{1}{2}\left(c_{j+1}^n + w_{j+1}^{n+1}\right)$.

The conditions on the corrections in this case are

$$-\theta \le \frac{\tilde{c}_{j+1}^{n,1} - \tilde{c}_j^n}{c_{j+1}^n - c_j^n}, \frac{\tilde{c}_{j+2}^n - \tilde{c}_{j+1}^{n,1}}{c_{j+2}^n - c_{j+1}^n} \le 1, \tag{65}$$

$$-\theta \le \frac{\tilde{c}_{j+1}^{n,2} - \tilde{\overline{c}}_j^{n+1/2}}{c_{j+1}^n - \overline{c}_j^{n+1/2}}, \frac{\tilde{c}_{j+2}^n - \tilde{c}_{j+1}^{n,2}}{c_{j+2}^n - c_{j+1}^n} \le 1, \tag{66}$$

$$-\theta \le \frac{\tilde{\bar{c}}^{n+1,1}_{j+1} - \tilde{c}^{n+1/2}_{j}}{\bar{c}^{n+1}_{j+1} - c^{n+1/2}_{j}}, \frac{\tilde{\bar{c}}^{n+1}_{j+2} - \tilde{\bar{c}}^{n+1,1}_{j+1}}{\bar{c}^{n+1}_{j+2} - \bar{c}^{n+1}_{j+1}} \le 1, \tag{67}$$

$$-\theta \le \frac{\tilde{\bar{c}}^{n+1}_{j+2} - \tilde{\bar{c}}^{n+1,2}_{j+1}}{\bar{c}^{n+1}_{j+2} - \bar{c}^{n+1}_{j+1}}, \frac{\tilde{\bar{c}}^{n+1,2}_{j+1} - \tilde{\bar{c}}^{n+1}_{j}}{\bar{c}^{n+1}_{j+1} - \bar{c}^{n+1}_{j}} \le 1. \tag{68}$$

These conditions lead to the following result. The proof is left to the reader.

PROPOSITION 3.3. *Assume a time step of size Δt^n for all elements to the right of $x_{j+1/2}$ and size $\Delta t^n/2$ for all elements to the left of $x_{j+1/2}$, where Δt^n satisfies* (48) *and* (49) *(with u replaced by $-u$). Then, for Scheme* II *above with $f(c) = uc$ where $u < 0$, with corrections satisfying* (65)–(68) *on I_j and I_{j+1} and* (5)–(6) *elsewhere, we have*

$$\sup_j |c^n_j| \le \sup_j |c^0_j|. \tag{69}$$

3.4. Extension to a nonlinear flux function. The extension of the methods above to a more general numerical flux h essentially combines the ideas of Schemes I and II above. In particular, the method is as follows.

Scheme III (general flux function).

(i) Compute corrections $\tilde{c}^n_{j-1}$, $\tilde{c}^n_j$, $\tilde{c}^{n,1}_{j+1}$, and $\tilde{c}^n_{j+2}$ so that (44) and (65) are satisfied.

(ii) $\bar{c}^{n+\frac{1}{2}}_j = c^n_j - \frac{\lambda^n_j}{2}[h(c^n_j + \tilde{c}^n_j, c_{j+1} - \tilde{c}^{n,1}_{j+1}) - h(c^n_{j-1} + \tilde{c}^n_{j-1}, c^n_j - \tilde{c}^n_j)]$.

(iii) Compute $\tilde{\bar{c}}^{n+1/2}_{j-1}$, $\tilde{\bar{c}}^{n+1/2}_j$, and $\tilde{c}^{n,2}_{j+1}$ so that (45) and (66) are satisfied.

(iv) Compute $w^{n+\frac{1}{2}}_j$ by

$$w^{n+\frac{1}{2}}_j = \bar{c}^{n+\frac{1}{2}}_j - \frac{\lambda^n_j}{2}\left[h(\bar{c}^{n+\frac{1}{2}}_j + \tilde{\bar{c}}^{n+\frac{1}{2}}_j, c^n_{j+1} - \tilde{c}^{n,2}_{j+1}) - h(\bar{c}^{n+\frac{1}{2}}_{j-1} + \tilde{\bar{c}}^{n+\frac{1}{2}}_{j-1}, \bar{c}^{n+\frac{1}{2}}_j - \tilde{\bar{c}}^{n+\frac{1}{2}}_j)\right].$$

(v) $c^{n+\frac{1}{2}}_j = \frac{1}{2}(c^n_j + w^{n+\frac{1}{2}}_j)$.

(vi) Define $\tilde{c}^n_{j+1} \equiv \frac{1}{2}(\tilde{c}^{n,1}_{j+1} + \tilde{c}^{n,2}_{j+1})$.

(vii) Compute $\bar{c}^{n+1}_{j+1}$ by

$$\bar{c}^{n+1}_{j+1} = c^n_{j+1} - \lambda^n_{j+1}\left[h(c^n_{j+1} + \tilde{c}^n_{j+1}, c^n_{j+2} - \tilde{c}^n_{j+2}) - \frac{1}{2}(h(c^n_j + \tilde{c}^n_j, c^n_{j+1} - \tilde{c}^{n,1}_{j+1}) + h(\bar{c}^{n+\frac{1}{2}}_j + \tilde{\bar{c}}^{n+\frac{1}{2}}_j, c^n_{j+1} - \tilde{c}^{n,2}_{j+1}))\right].$$

(viii) Compute $\tilde{c}^{n+\frac{1}{2}}_{j-1}$, $\tilde{c}^{n+\frac{1}{2}}_j$, $\tilde{\bar{c}}^{n+1,1}_{j+1}$, and $\tilde{\bar{c}}^{n+1}_{j+2}$ so that (46) and (67) are satisfied.

(ix) Compute $\bar{c}^{n+1}_j$ by

$$\bar{c}^{n+1}_j = c^{n+\frac{1}{2}}_j - \frac{\lambda^n_j}{2}\left[h(c^{n+\frac{1}{2}}_j + \tilde{c}^{n+\frac{1}{2}}_j, \bar{c}^{n+1}_{j+1} - \tilde{\bar{c}}^{n+1,1}_{j+1}) - h(c^{n+\frac{1}{2}}_{j-1} + \tilde{c}^{n+\frac{1}{2}}_{j-1}, c^{n+\frac{1}{2}}_j - \tilde{c}^{n+\frac{1}{2}}_j)\right].$$

(x) Compute $\tilde{\bar{c}}^{n+1}_{j-1}$, $\tilde{\bar{c}}^{n+1}_j$, and $\tilde{\bar{c}}^{n+1,2}_{j+1}$ so that (47) and (68) are satisfied.

(xi) Compute w^{n+1}_j by

$$w^{n+1}_j = \bar{c}^{n+1}_j - \frac{\lambda^n_j}{2}\left[h(\bar{c}^{n+1}_j + \tilde{\bar{c}}^{n+1}_j, \bar{c}^{n+1}_{j+1} - \tilde{\bar{c}}^{n+1,2}_{j+1}) - h(\bar{c}^{n+1}_{j-1} + \tilde{\bar{c}}^{n+1}_{j-1}, \bar{c}^{n+1}_j - \tilde{\bar{c}}^{n+1}_j)\right].$$

(xii) $c^{n+1}_j = \frac{1}{2}(c^{n+\frac{1}{2}}_j + w^{n+1}_j)$.

(xiii) Define $\tilde{\bar{c}}_{j+1}^{n+1} \equiv \frac{1}{2}(\tilde{\bar{c}}_{j+1}^{n,1} + \tilde{\bar{c}}_{j+1}^{n,2})$.
(xiv)

$$w_{j+1}^{n+1} = \bar{c}_{j+1}^{n+1} - \frac{\Delta t^n}{\Delta x_{j+1}} \left[h(\bar{c}_{j+1}^{n+1} + \tilde{\bar{c}}_{j+1}^{n+1}, \bar{c}_{j+2}^{n+1} - \tilde{\bar{c}}_{j+2}^{n+1}) \right.$$
$$\left. -\frac{1}{2}\left(h(c_j^{n+\frac{1}{2}} + \tilde{c}_j^{n+\frac{1}{2}}, \bar{c}_{j+1}^{n+1} - \tilde{\bar{c}}_{j+1}^{n+1,1}) + h(\bar{c}_j^{n+1} + \tilde{\bar{c}}_j^{n+1}, \bar{c}_{j+1}^{n+1} - \tilde{\bar{c}}_{j+1}^{n+1,2}) \right) \right].$$

(xv) $c_{j+1}^{n+1} = \frac{1}{2}\left(c_{j+1}^n + w_{j+1}^{n+1}\right)$.

3.5. Extension to *M* steps. Now suppose we take M steps in grid block I_j to one step in block I_{j+1}. The easier extension of the method described above is for the case where M is even, although an extension to M odd can also be made.

Assume M is even. When $M = 2$, note that to compute $\bar{c}_{j+1}^{n+1}$ we used the values c_j^n up through $\bar{c}_j^{n+1/2}$. The same is true in general. We compute $\bar{c}_j^{n+1/2}$ by taking $M/2$ steps in block I_j. The average of the fluxes along edge $j + 1/2$ over these steps is used to compute $\bar{c}_{j+1}^{n+1}$, just as above. The computation of w_{j+1}^{n+1} is analogous. We take $M/2$ steps to compute $\bar{c}_{j+1}^{n+1}$, starting with $c_j^{n+1/2}$, and the average of the fluxes along edge $j + 1/2$ is used to compute w_{j+1}^{n+1}.

The maximum principle argument can be carried through with appropriate limiting of the corrections. Similar to the case $M = 2$, at each substep i, $i = 1, \ldots, M/2$, we compute a correction $\tilde{c}_{j+1}^{n,i}$ in block I_{j+1} so that the analogues of (44), (45), (65), and (66) are satisfied. The final correction $\tilde{c}_{j+1}^n$ is the average of all of these substep corrections. Similarly, once $\bar{c}_{j+1}^{n+1}$ is computed, corrections $\tilde{\bar{c}}_{j+1}^{n+1,i}$ are computed at each substep so that the analogues of (46), (47), (67), and (68) are satisfied, and $\tilde{\bar{c}}_{j+1}^{n+1}$ is computed by averaging these corrections.

4. Numerical results. Here we present results examining the accuracy and stability of the method in section 3.

4.1. Linear example: Smooth problem. We will first show how local time stepping affects the errors and stability in the case of a smooth linear problem. Consider initial and boundary conditions such that the true solution is $\sin(\pi(x-t))$. The space-time domain is $[0,1]^2$. We have the following cases:

1. Uniform mesh of width Δx, global time step $\Delta t = \frac{2\Delta x}{3}$.
2. Region $[0, 0.5]$ refined to $\frac{\Delta x}{2}$, time step globally refined to $\Delta t = \frac{\Delta x}{3}$.
3. Region $[0, 0.5]$ refined to $\frac{\Delta x}{2}$, time step on $[0, 0.5]$ reduced (locally) by a factor of 2.

Examining Tables 1, 2, and 3, we see that the rate of convergence in L^2 in all three cases is around 1.5, which is to be expected for a *minmod*-limited method. Conceivably, the local time stepping could incur an $\mathcal{O}(h^{\frac{1}{2}})$ error which a constant time step would not incur. Thus, we turned off the limiter on the slopes and saw that the local stepping does not degenerate the order of accuracy, as we see second order convergence in Tables 4 and 5.

4.2. Linear example: Rough problem. Now that we have seen that the local time stepping scheme does not degenerate the accuracy of the approximation, we will show that the method is indeed stable with a local CFL condition. Consider the linear model case of $f(c) = c$ with $c(x, 0) = 1$ for $x < 0$ and $c(x, 0) = 0$ for $x > 0$. At $t = 0.5$, the true solution is a front at $x = 0.5$. Consider the following situations:

TABLE 1
Case 1: *Uniform mesh, global time step.*

Δx	L^2 error	L^1 error
.2500D+00	.1447D+00	.1205D+00
.1250D+00	.4995D-01	.3827D-01
.6250D-01	.1821D-01	.1422D-01
.3125D-01	.6033D-02	.4248D-02
.1562D-01	.1955D-02	.1287D-02
.7812D-02	.6291D-03	.3714D-03
rate:	1.56	1.66

TABLE 2
Case 2: *Local refinement, global time step.*

Δx	L^2 error	L^1 error
.2500D+00	.1145D+00	.9424D-01
.1250D+00	.4116D-01	.2646D-01
.6250D-01	.1461D-01	.8774D-02
.3125D-01	.4869D-02	.2550D-02
.1562D-01	.1586D-02	.7236D-03
.7812D-02	.5112D-03	.1965D-03
rate:	1.56	1.77

TABLE 3
Case 3: *Local refinement, local time step.*

Δx	L^2 error	L^1 error
.2500D+00	.1306D+00	.1030D+00
.1250D+00	.4304D-01	.2641D-01
.6250D-01	.1620D-01	.1018D-01
.3125D-01	.5981D-02	.3328D-02
.1562D-01	.2128D-02	.1052D-02
.7812D-02	.7441D-03	.3196D-03
rate:	1.48	1.63

TABLE 4
Uniform mesh and time step on $[0, 1]$, *unlimited slopes.*

Δx	L^2 error	L^1 error
.2500D+00	.1380D+00	.1317D+00
.1250D+00	.4331D-01	.3371D-01
.6250D-01	.1147D-01	.9483D-02
.3125D-01	.2869D-02	.2417D-02
.1562D-01	.7079D-03	.6061D-03
.7812D-02	.1746D-03	.1509D-03
rate:	1.94	1.95

TABLE 5
Uniform mesh and local time step on $[0, 1]$, *unlimited slopes.*

Δx	L^2 error	L^1 error
.2500D+00	.1290D+00	.1113D+00
.1250D+00	.3908D-01	.2951D-01
.6250D-01	.9640D-02	.7284D-02
.3125D-01	.2235D-02	.1785D-02
.1562D-01	.5294D-03	.4355D-03
.7812D-02	.1281D-03	.1078D-03
rate:	2.02	2.01

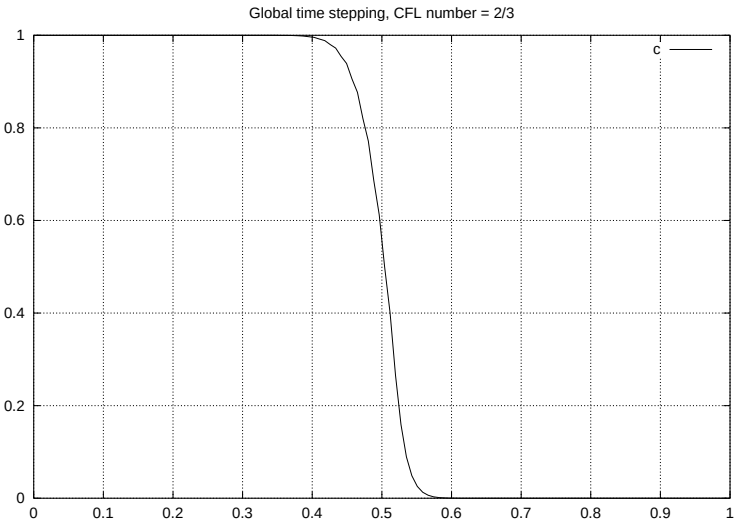

FIG. 3. *Global time stepping, model advective front.*

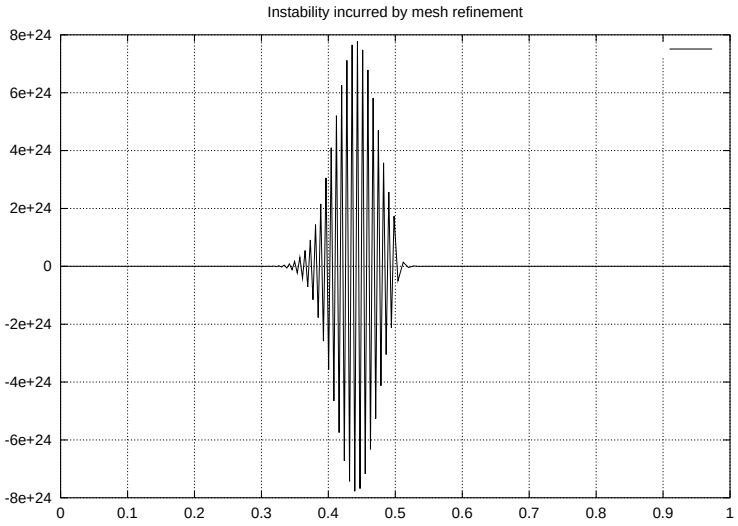

FIG. 4. *Local mesh refinement creates instability.*

1. Global uniform mesh, $\Delta x = \frac{1}{128}$, global CFL number of $\frac{2}{3}$.
2. Refine the mesh on $[0, 0.5]$ by a factor of 2, keep the same global time step. (CFL number in first half of the domain is $\frac{4}{3}$.)
3. Refine the time step on $[0, 0.5]$ by a factor of 2, giving a *local* CFL number of $\frac{2}{3}$ everywhere.

Observe that the front is propagated stably in the first case in Figure 3 but when the CFL condition is violated in the second case, we incur massive instability (Figure 4). However, the local time stepping method, with its local CFL condition, gives a stable and accurate approximation to the front in Figure 5.

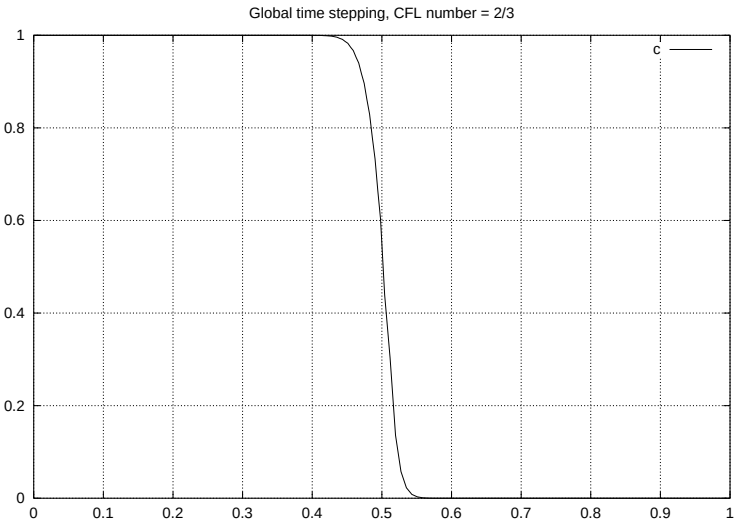

FIG. 5. *Local time stepping restores stability.*

4.3. Nonlinear example: Buckley–Leverett. Next, we examine a case where the flux is nonlinear. The Buckley–Leverett problem, given by

$$f(c) = \frac{c^2}{c^2 + a(1-c)^2}, \tag{70}$$

is a standard test problem arising in two-phase flow in porous media. This flux function is Lipschitz but nonconvex. In the case of $a = 0.25$, it is known from the Rankine–Hugoniot condition that the front is a rarefaction down to the point where $c = 0.44$, and then the solution jumps to $c = 0$. See, for example, [10] for a discussion. The Rankine–Hugoniot condition also gives that this front propagates at a velocity of 1.62. We performed a series of numerical experiments on a uniform mesh. First, we used global time stepping to verify that the code put the shock in the right location with the correct jump. Then, we refined the time step in the first half of the domain repeatedly in order to verify that the local time stepping did not alter the method's shock-capturing abilities. Each of these cases was run with a mesh spacing of $\Delta x = \frac{1}{128}$ and a main time step of $\Delta t = \frac{1}{160}$ to time $t = 0.5$. The true front should be at $x = 0.81$. These fronts were all near, though diffused, and further spatial refinements gave sharper fronts at the right spot. Figure 6 shows these results.

Further, we show that we have stability only subject to a local CFL constraint. Again, we consider three cases, with $\Delta x_{\max} = \frac{1}{128}$ and $\Delta t_{\max} = \frac{1}{160}$. In each case, the mesh width is $\frac{1}{2}\Delta x_{\max}$ on $[0, 0.5]$ and $\Delta x_{\max}$ elsewhere.

1. Global time step $\Delta t_{\max}$.
2. Global time step $\frac{1}{2}\Delta t_{\max}$.
3. Local time stepping.

As seen in Figure 7, the large time step in the presence of the local refinement has caused some mild instability with over- and undershoot. Due to the large velocity, this mild oscillation has propagated out of the first part of the domain and into the second. However, when the time step is refined either globally or locally in the presence of the mesh refinement, the front is well approximated.

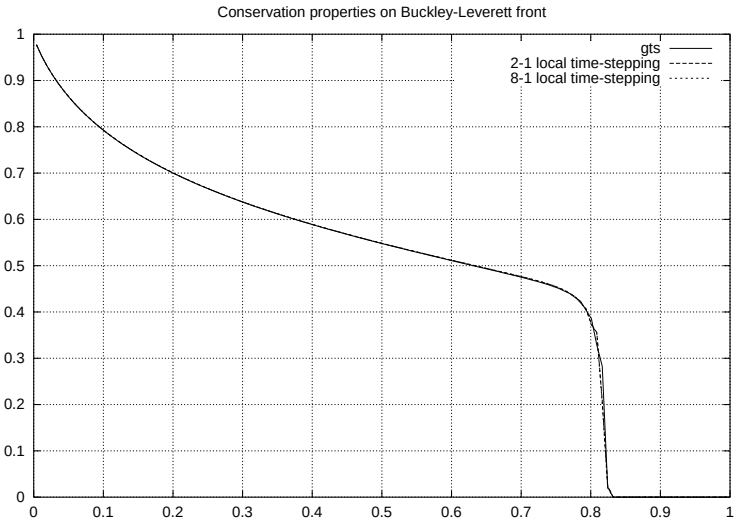

FIG. 6. *Local time stepping approximations to Buckley–Leverett front at* $x = 0.81$.

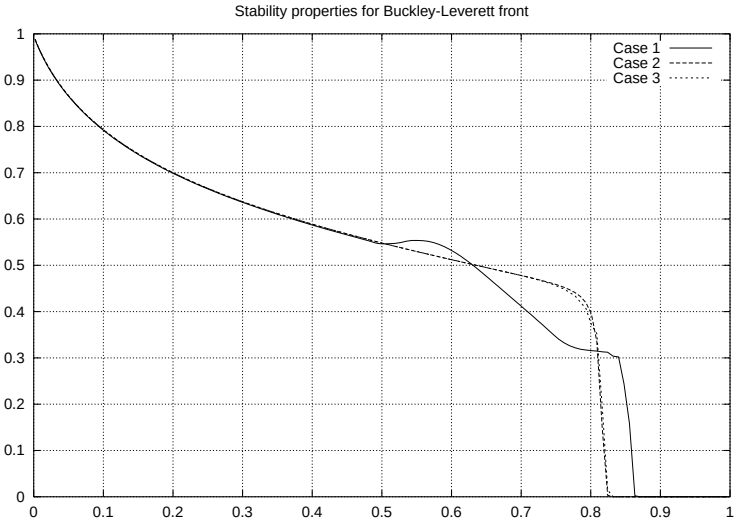

FIG. 7. *Local time stepping cures instability caused by local mesh refinement.*

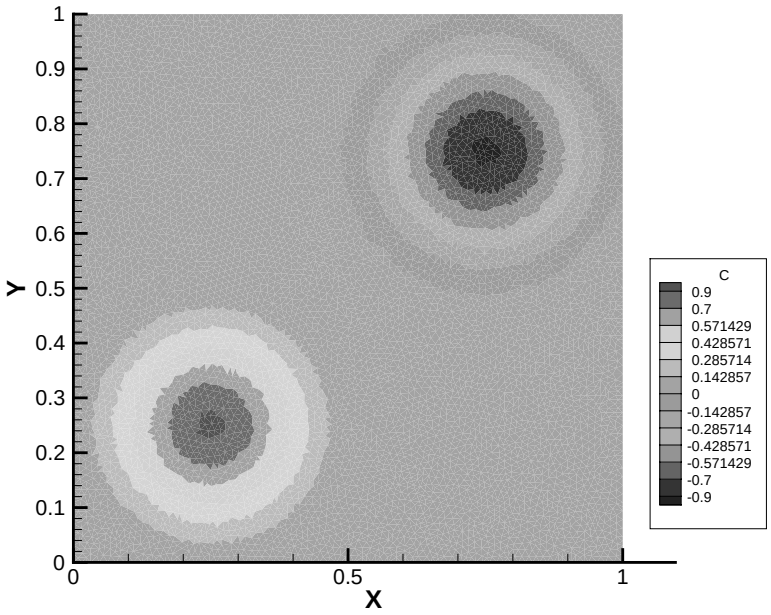

FIG. 8. *Initial condition for Burgers' equation, consisting of a cone of height* 1 *in the lower left corner, and a cone of height* -1 *in the upper right corner.*

5. Two-dimensional Burgers' equation. The local time stepping schemes described above have been extended to two space dimensions. The spatial discretization we have employed is based on a high resolution method developed by Durlofsky, Engquist, and Osher [4] for unstructured, triangular grids. The difference between what we have implemented and the method in [4] is in the slope-limiting step. Three different slopes are constructed using linear interpolation with the element and its neighbors. Then the steepest slope which does not introduce overshoot/undershoot at the edge boundaries is selected. The two methods differ in the case where no slopes satisfy this condition. In our implementation, the slope is set to zero in this case, whereas Durlofsky, Engquist, and Osher simply choose the interpolant with the smallest gradient.

Some results for local time stepping applied to the transport equation (1), with highly varying velocity fields, can be found in [9]. Here, we apply local time stepping to the two-dimensional inviscid Burgers' equation

$$c_t + f(c)_x + f(c)_y = 0, \tag{71}$$

where $f(c) = \frac{c^2}{2}$. We take as an initial condition a function consisting of two cone shapes, one with height 1 and the other with height -1. The initial condition is displayed in Figure 8.

In Burgers' equation, larger concentrations give rise to larger velocities. Consequently, the centers of the cones are advected along at a higher rate than the edges. Moreover, the positive cone has positive velocity and the negative cone negative velocity; thus, the cones approach each other and "collide" in the center of the domain. This general behavior is given in Figure 9, where we have shown the solution at time

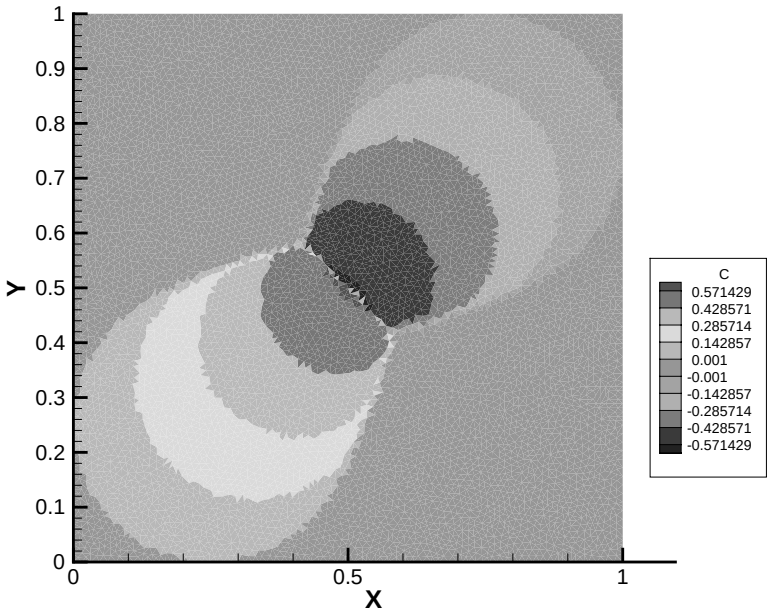

FIG. 9. *Global time stepping solution at* $T = 1.1$.

$T = 1.1$. This solution was obtained using the method in [4], modified as mentioned above, with Heun's method used for the temporal integration. The finite element mesh for this case, shown in Figure 10, consists of 15489 triangles and is unstructured.

An extension of the second order local time stepping scheme described previously was implemented for this problem. In our implementation, the elements take either the global CFL time step or a time step M times larger, assuming that this larger time step does not violate the local CFL constraint. The time steps are redistributed throughout the domain after each large time step. Numerical results for $M = 2$, 5, and 10 were generated. Relative L^1 and L^2 errors between the local and global time stepping solutions were computed at time $T = 1.1$. The relative L^1 error is

$$Error_{L^1} = \frac{\sum_E |c_{global}(x_E) - c_{local}(x_E)|m(E)}{\sum_E |c_{global}(x_E)|m(E)}, \tag{72}$$

where the sum on E is over all elements, x_E is the barycenter of element E, c_{global} is the global time stepping solution, c_{local} is the local time stepping solution, and $m(E)$ is the area of triangle E. A similar definition holds for the relative L^2 error. These errors are given in Table 6. Note that they are on the order of 1%.

Table 7 shows the CPU run times in seconds for each of these cases. Notice a speedup of about 1.7–2.4 for the M:1 time stepping scheme over the global time stepping scheme. For this problem, most elements near the peaks of the cones take the smaller (global CFL) time step, as these elements have larger velocity. As the simulation proceeds, the solution spreads and eventually more elements are forced to take the smaller time step. This phenomenon is seen in Figures 11 and 12, where the local time step distribution is plotted at times $T = .1$ and $T = 1.1$, respectively, for the case $M = 5$. For the $M = 10$ case, the small time step region is more extensive, because fewer elements meet the criterion necessary to take the larger time step. Thus, any gains in increasing M are offset somewhat, and consequently there

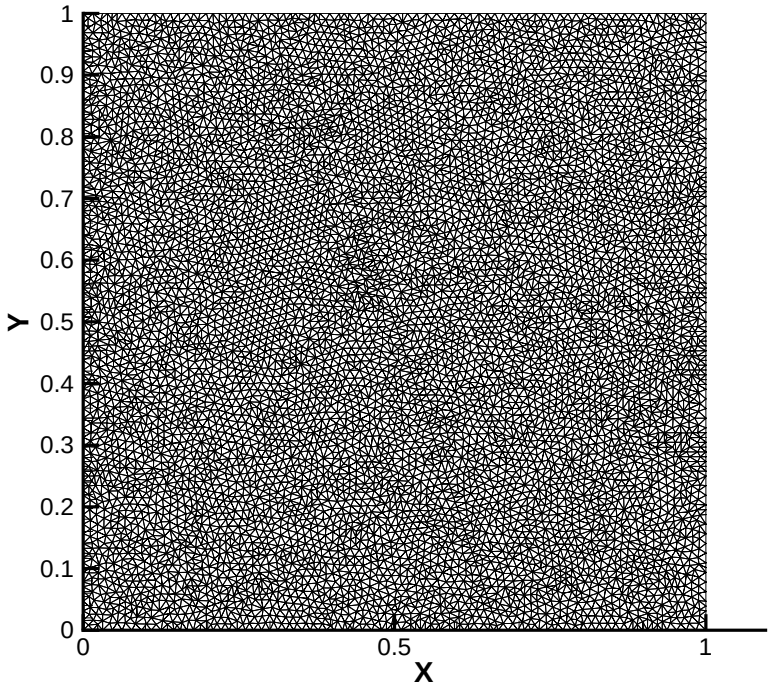

FIG. 10. *Finite element mesh for Burgers' equation test case.*

TABLE 6
Relative L^1 and L^2 errors for M:1 time stepping schemes.

M	Rel. L^1 error	Rel. L^2 error
2	.0041	.0130
5	.0044	.0086
10	.0040	.0074

TABLE 7
Transport run times in seconds for M:1 time stepping schemes.

M	Run time (sec)
1	2533
2	1480
5	1116
10	1075

is not a dramatic decrease in run time as we increase M for this problem. In Figure 13, we have plotted the percentage of elements taking the global CFL time step vs. simulation time for $M = 2$, 5, and 10. Here we see that for $M = 2$, initially about 3.5% of the elements take the global CFL time step, and the percentage grows to about 7% by the final time, $T = 1.1$. For $M = 5$, the range is from about 20% to 27%, and for $M = 10$, the range is about 28% to 37%. For M too large, of course, all elements would be forced to take the global CFL time step.

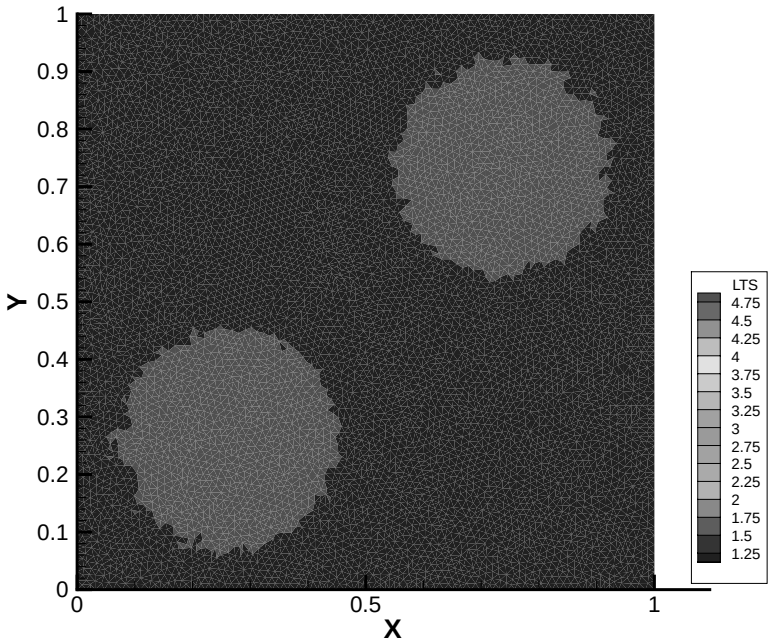

FIG. 11. *Distribution of local time steps for $M = 5$ and $T = .1$. Lighter region indicates where smaller time steps were taken.*

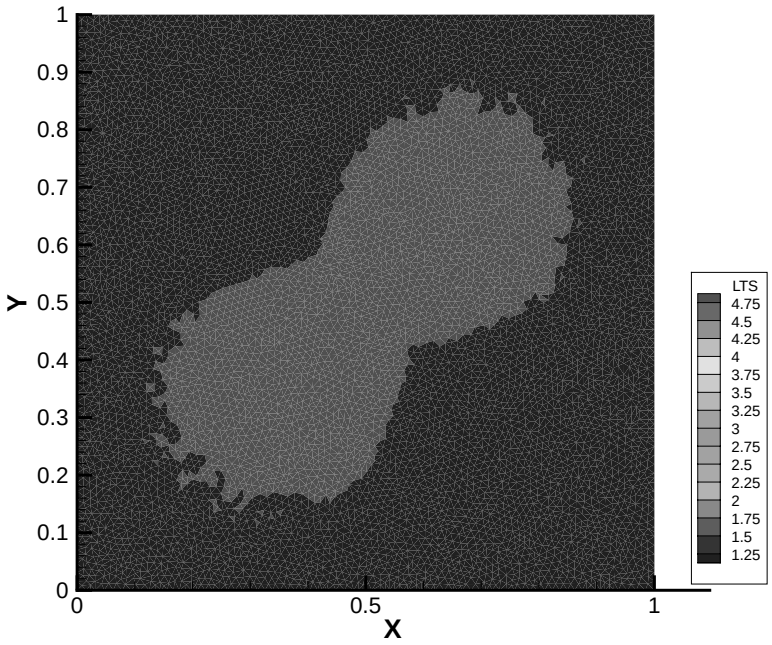

FIG. 12. *Distribution of local time steps for $M = 5$ and $T = 1.1$. Lighter region indicates where smaller time steps were taken.*

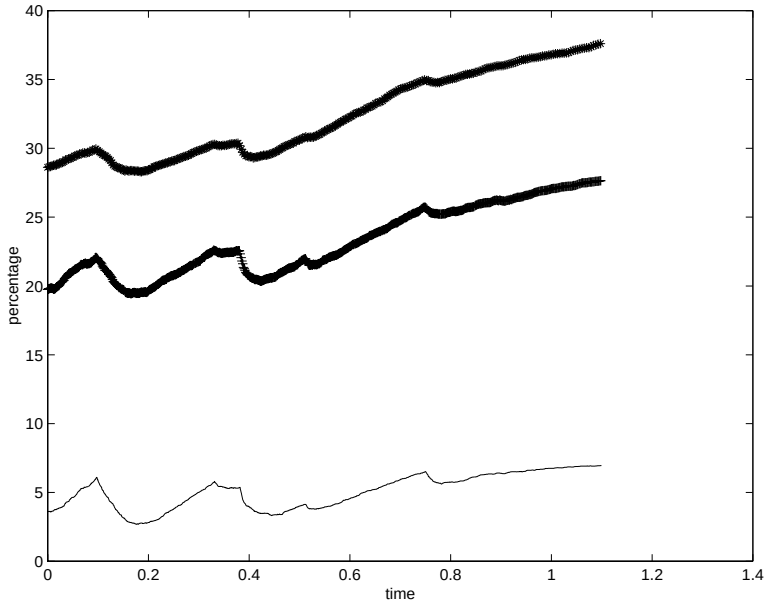

FIG. 13. *Percentage of elements taking the global CFL time step as a function of simulation time for $M = 2$ (solid line), $M = 5$ (+), and $M = 10$ (*).*

6. Conclusions. We have developed and proved maximum principles for local time stepping schemes based on first and second order time discretizations, and piecewise linear spatial discretizations. Numerical results given here and in [9] indicate that these local time stepping schemes exhibit similar accuracy and stability to the global time stepping schemes upon which they are based, at a fraction of the computational cost.

In this paper, we have not addressed the issue of whether our local time stepping schemes satisfy additional properties (TVB, etc.) from which we could conclude that the schemes converge to the entropy solution. However, all of our numerical results to date indicate that the local time stepping solutions are almost identical to those obtained by global time stepping. Thus, our experiences so far lead us to believe that our local time stepping schemes inherit the convergence properties of the related global scheme, though this has not been proven.

REFERENCES

[1] M. BERGER AND J. OLIGER, *Adaptive mesh refinement for hyperbolic partial differential equations*, J. Comput. Phys., 53 (1984), pp. 484–512.

[2] B. COCKBURN AND C.-W. SHU, *TVB Runge-Kutta local projection discontinuous Galerkin finite element method for scalar conservation laws* II: *General framework*, Math. Comp., 52 (1989), pp. 411–435.

[3] C. DAWSON, *High resolution upwind-mixed finite element methods for advection-diffusion equations with variable time-stepping*, Numer. Methods Partial Differential Equations, 11 (1995), pp. 525–538.

[4] L. DURLOFSKY, B. ENGQUIST, AND S. OSHER, *Triangle based adaptive stencils for the solution of hyperbolic conservation laws*, J. Comput. Phys., 98 (1992), pp. 64–73.

[5] J. E. FLAHERTY, R. M. LOY, M. S. SHEPHARD, B. K. SZYMANSKI, J. D. TERESCO, AND L. H. ZIANTZ, *Adaptive local refinement with octree load-balancing for the parallel solution of three-dimensional conservation laws*, Journal of Parallel and Distributed Computing, 47 (1997), pp. 139–152.

[6] S. Gottlieb and C.-W. Shu, *Total variation diminishing Runge-Kutta schemes*, Math. Comp., 67 (1998), pp. 73–85.
[7] A. Harten and S. Osher, *Uniformly high-order accurate nonoscillatory schemes.* I, SIAM J. Numer. Anal., 24 (1987), pp. 279–309.
[8] J. Kallinderis and J. Baron, *Adaptation methods for viscous flows*, in Computational Methods in Viscous Aerodynamics, C. A. Brebbia, ed., Elsevier, Amsterdam, 1990.
[9] R. Kirby, *A Posteriori Error Estimates and Local Time-Stepping for Flow and Transport Problems in Porous Media*, Ph.D. thesis, University of Texas at Austin, Austin, TX, 2000.
[10] R. Leveque, *Numerical Methods for Conservation Laws*, Birkhäuser-Verlag, Boston, 1990.
[11] S. Osher and R. Sanders, *Numerical approximations to nonlinear conservation laws with locally varying time and space grids*, Math. Comp., 41 (1983), pp. 321–336.
[12] C.-W. Shu, *TVB uniformly high-order schemes for conservation laws*, Math. Comp., 49 (1987), pp. 105–121.
[13] C.-W. Shu, *Total-variation-diminishing time discretizations*, SIAM J. Sci. Statist. Comput., 9 (1988), pp. 1073–1084.
[14] B. van Leer, *Towards the ultimate conservative difference scheme,* V. *A second order sequel to Godunov's method*, J. Comput. Phys., 32 (1979), pp. 101–136.